Electronic Supplementary Material (ESI) for Catalysis Science & Technology.

# Electronic Supporting Information

## Kinetic Monte Carlo simulations of the Dry Reforming of Methane catalyzed by the Ru (0001) surface based on Density Functional Theory calculations

Estefanía Díaz López[1] and Aleix Comas-Vives[1,2]*

[1]*Department of Chemistry, Universitat Autònoma de Barcelona, 08193 Cerdanyola del Vallès, Catalonia, Spain*

[2]Institute of Materials Chemistry, TU Wien, 1060 Vienna, Austria.

e-mail: aleix.comas@tuwien.ac.at, aleix.comas@uab.cat

**Equation used for gas-phase species involved in the DRM mechanism:**

The partition function for $X_{(gas)}$ was written as:

$$Q_{X_{gas}} = q_{X_{gas},vib} \cdot q_{X_{gas},rot} \cdot q_{X_{gas},trans3D} \qquad (1)$$

The distance of $X_{(gas)}$ from the surface can be used as a reaction coordinate, thereby motivating the decoupling of the z component of the translational partition function as follows:

$$q_{X_{gas},trans3D} = q_{X_{gas},trans2D} \cdot l_z \cdot \frac{\sqrt{2 \cdot \pi \cdot m_X \cdot k_B \cdot T}}{h} \qquad (2)$$

Where $l_z$ the length of the gas-phase in the z-direction and the 2D translational partition function over a unit cell of the surface is:

$$q_{X_{gas},trans2D} = A_{st} \cdot \frac{2 \cdot \pi \cdot m_X \cdot k_B \cdot T}{h^2} \qquad (3)$$

Where $A_{st}$ corresponds to the effective area of the catalytic site (s) and $m_X$ is the mass of the adsorbing molecule. $A_{st}$ was calculated as the total area divided by the number of sites. The partition functions used for the gas-phase species ($Q_{vib}$ and $Q_{rot}$) were calculated with Gaussian 09 at PBE/6-311G(d,p) level.

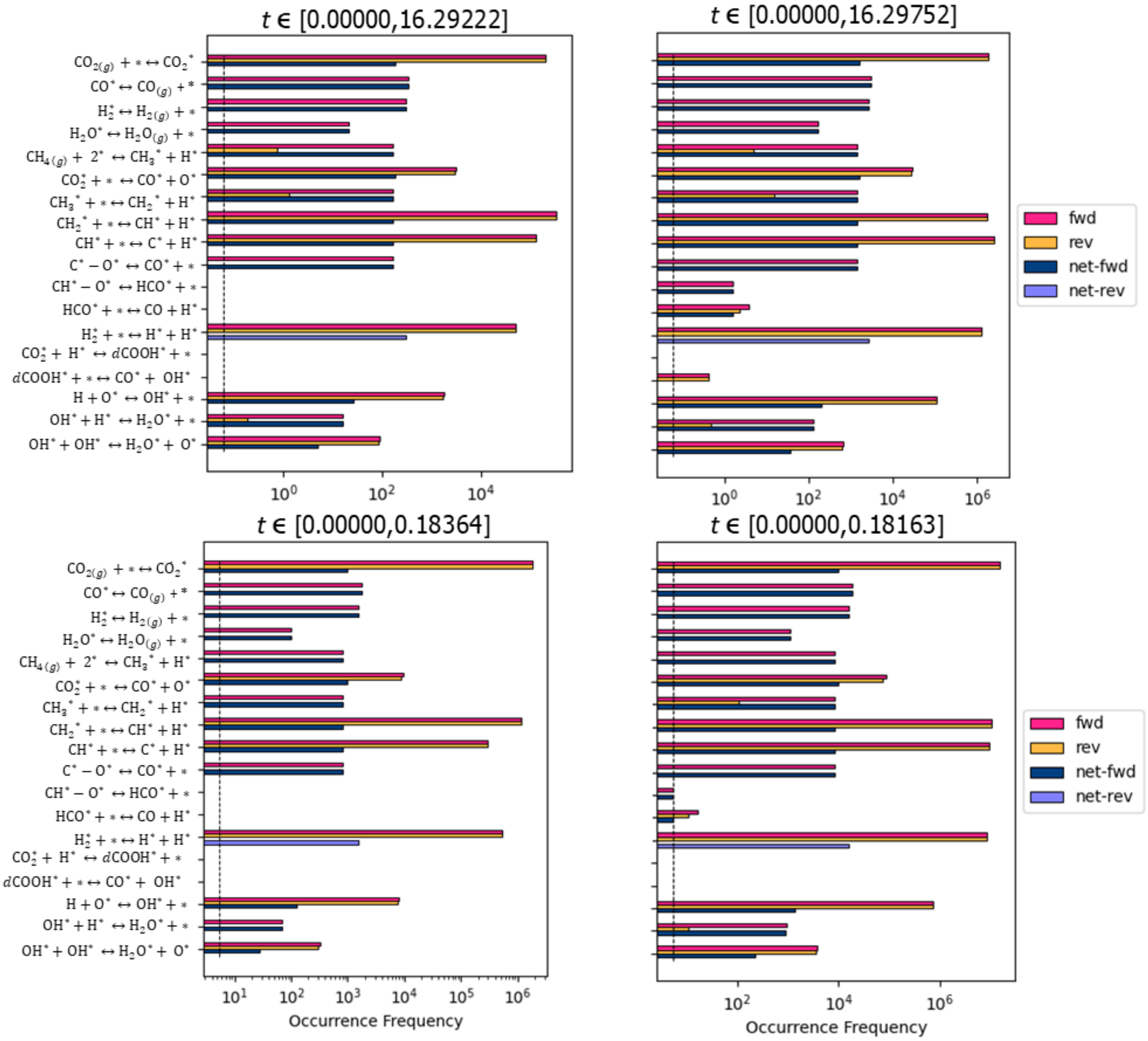

**Figure S1a**. Comparison of the main elementary processes and their frequencies for the DRM on Ru (0001) at $P_{CH_4}$= 0.16 kPa and $P_{CO_2}$= 0.16 kPa and T = 700 K (top) and T = 800 K (bottom) between a 5 × 5 lattice (left) and a 15 × 15 lattice (right).

Note: We obtained similar results for *k*MC simulations at 700 and 800 K of temperature and 0.32 kPa of total pressure with a 5 × 5 and 15 × 15 lattices and comparable simulation times. The most remarkable difference between the different lattice sizes is that the events become more frequent at bigger lattice sizes since there are more sites where elementary reactions can occur. Therefore, the probability of low occurrence events increases. Thus, HCO* forms and dissociates before for the large unit cell than for the small one. However, such processes also occur for the small unit cell at longer simulation times (see Figure 7, right, of the main text). There is a slight difference between the results obtained with a 5 × 5 lattice compared to the 15 × 15 one, which is the CH* dissociation process is more frequent with the 15 × 15 lattice for both temperatures. Nevertheless, this difference does not affect the main results; the TOF obtained at 700 K for both lattice sizes, 5 × 5 and 15 × 15, 2.29 and 2.25, respectively, at 800 K (1.29E+01 and 1.35E+01, respectively), are very close between them. Thereby, we can conclude our results are not depending on the lattice size.

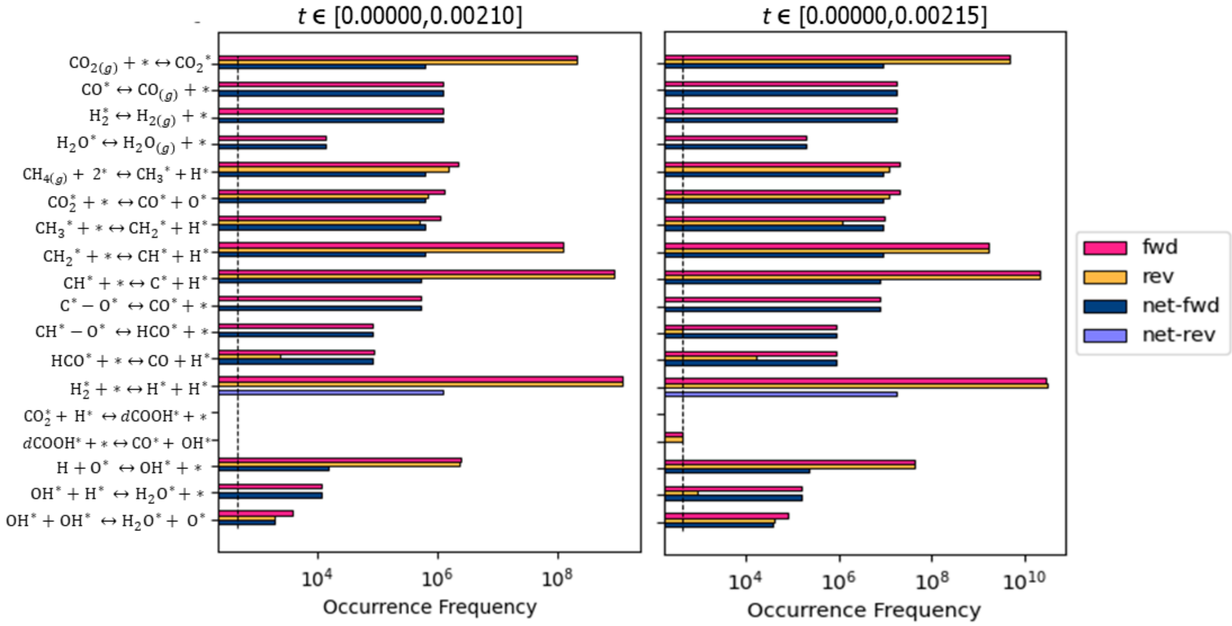

**Figure S1b.** Comparison of the main elementary processes and their frequencies for the DRM on Ru (0001) at $P_{CH_4}$= 50 kPa and $P_{CO_2}$= 50 kPa and T = 973 K for a 5 x 5 lattice (left) and a 15 x 15 lattice (right).

Note: We found comparable results to the former case, i. e., when increasing the lattice size, more events happen because there are more possibilities available. However, the TOF is slightly higher for the 15 × 15 than for the 5 × 5 lattice, i. e. 1.31E+04 and 7.28E+03, respectively. Thus, for the 15 × 15 lattice, the system is more active, although the $H_2$/CO ratio is practically the same for both lattice sizes (0.99 and 0.98, respectively). It is worth mentioning that the 5 × 5 deactivates faster than the 15 × 15 lattice. As a result, the latter's activity is slightly higher than the former.

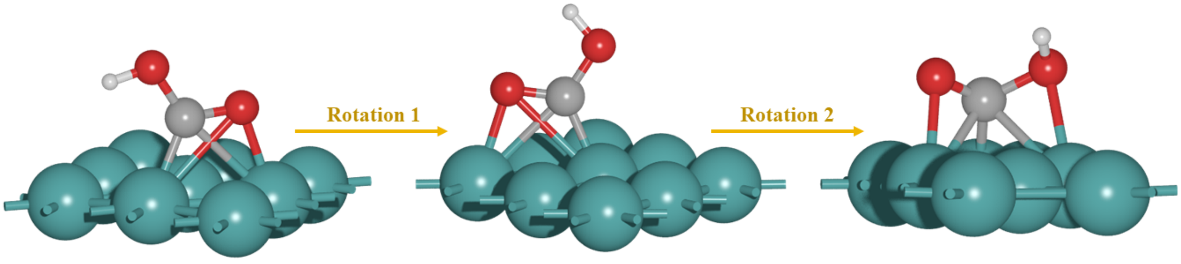

*d*-COOH *u*-COOH COOH-*tridentate*

**Figure S2.** Configurations for the carboxyl intermediate before its cleavage into CO* + OH* calculated with PBE functional.

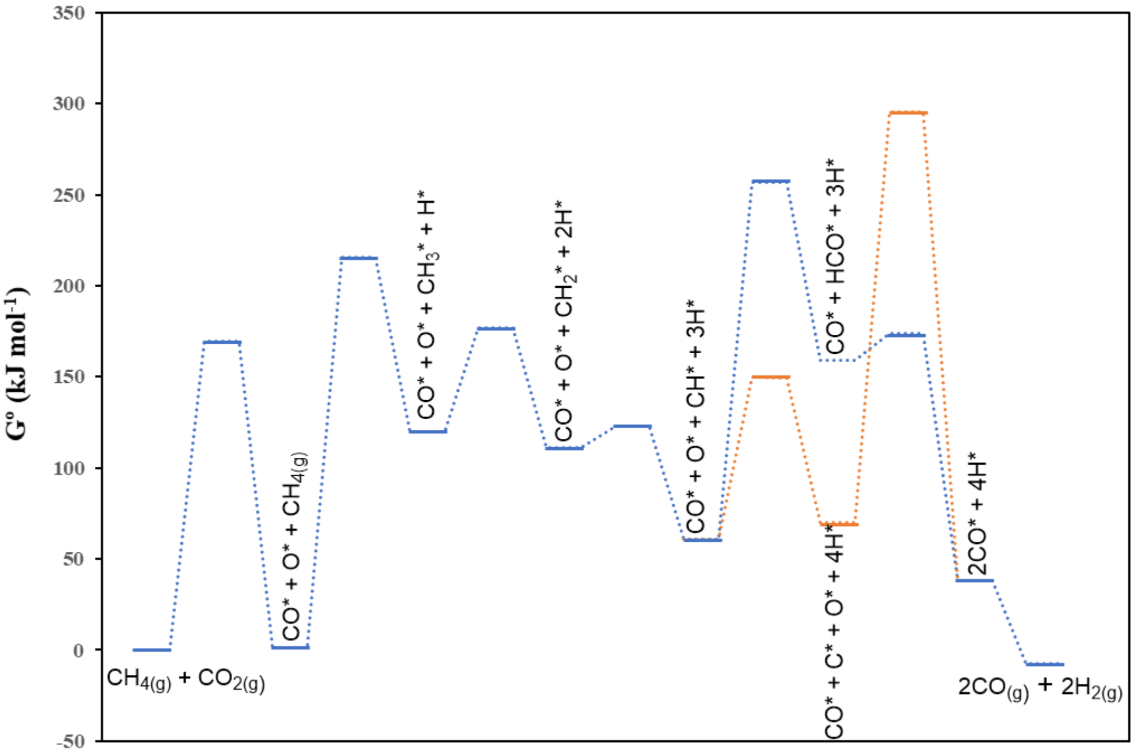

**Figure S3.** Free energy profile of DRM on Ru (0001) surface via CH-O oxidation (blue) and C-O oxidation (orange) at 973.15 K calculated with BEEF-vdW functional.

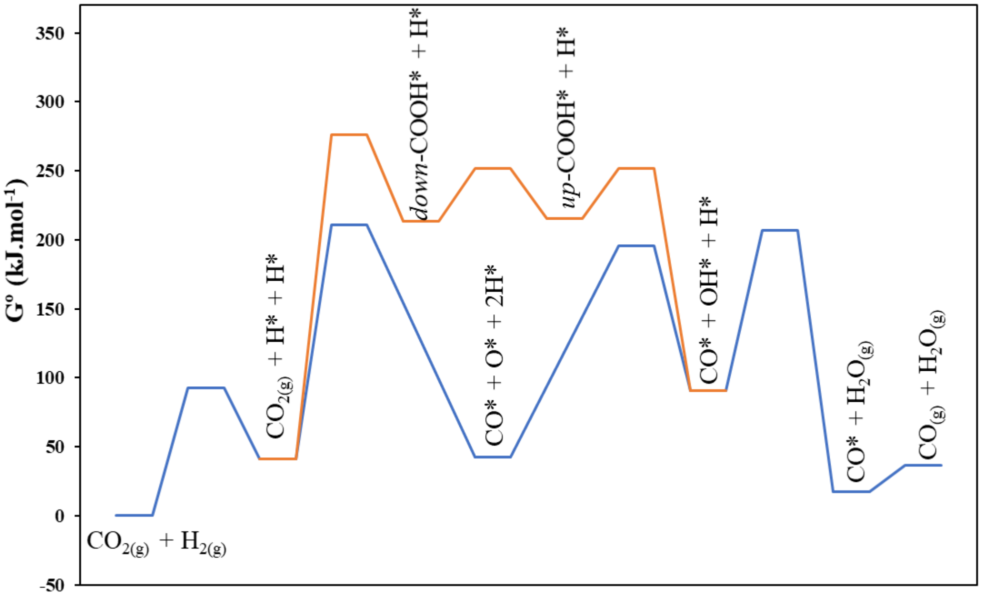

**Figure S4.** Free energy profile of reverse water gas shift reaction on Ru (0001) surface at 973.15 K calculated with BEEF-vdW functional.

*Graph pattern of the DRM elementary reactions used in the kMC simulations:*

1. **$CO_2$* activation**

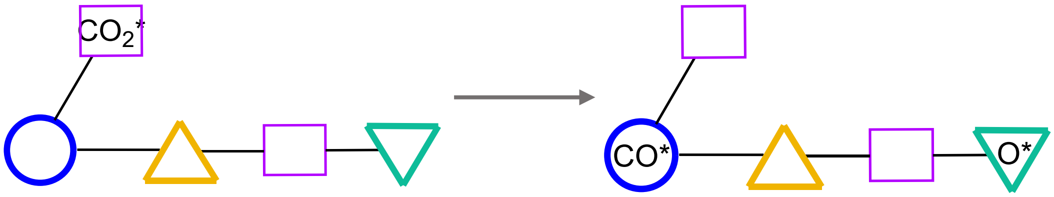

2. **$CH_4$ dissociative adsorption**

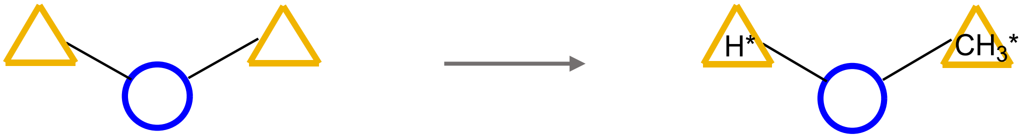

3. **$CH_3$* dissociation**

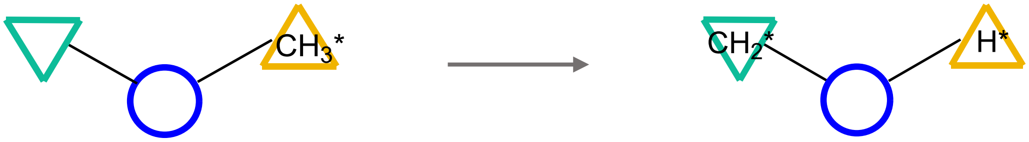

4. **$CH_2$* dissociation**

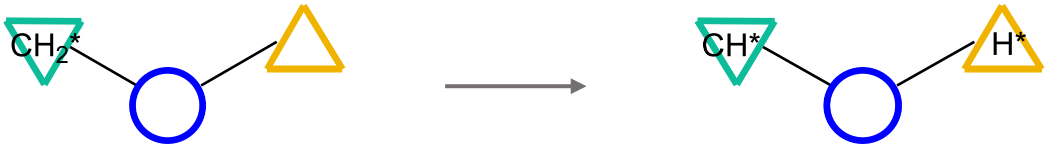

5. **CH* dissociation**

6. **CO* formation**

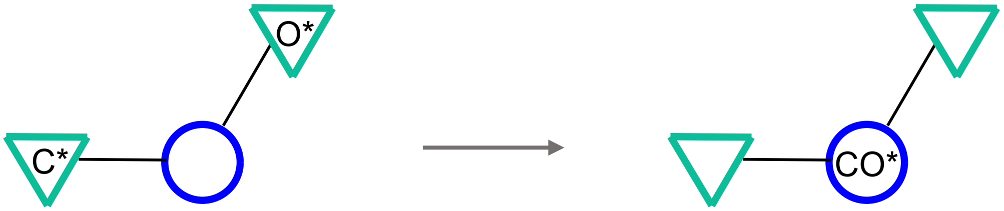

7. **HCO* formation**

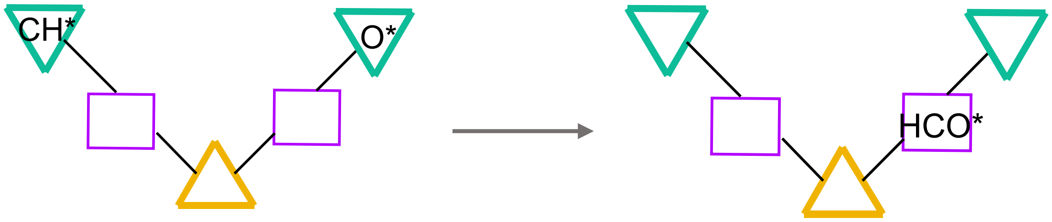

8. **HCO* dissociation**

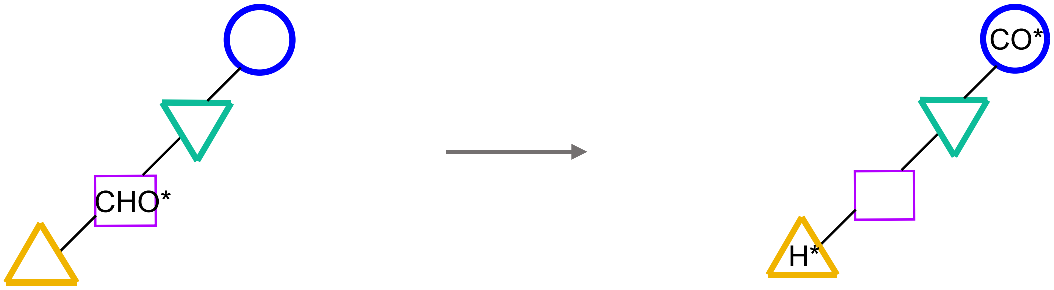

9. **$H_2$* dissociation**

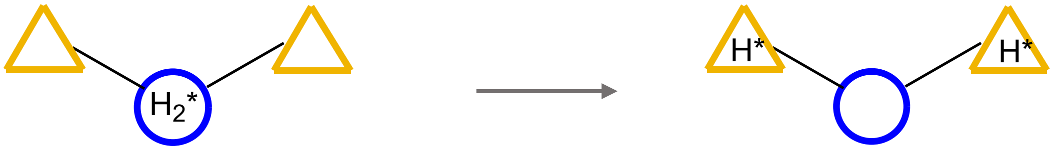

### 10. *down*-COOH* formation

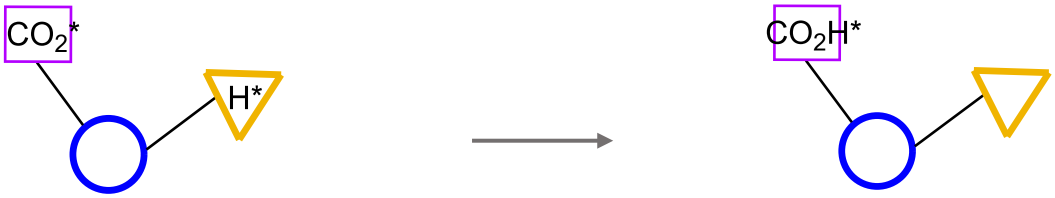

### 11. *down*-COOH* dissociation

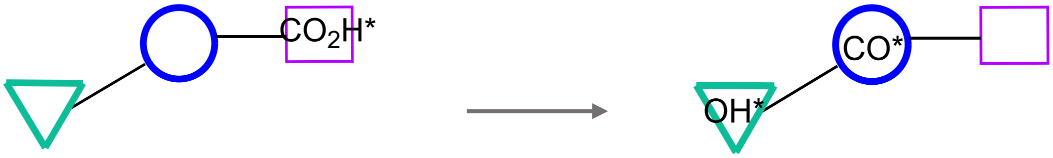

### 12. OH* formation

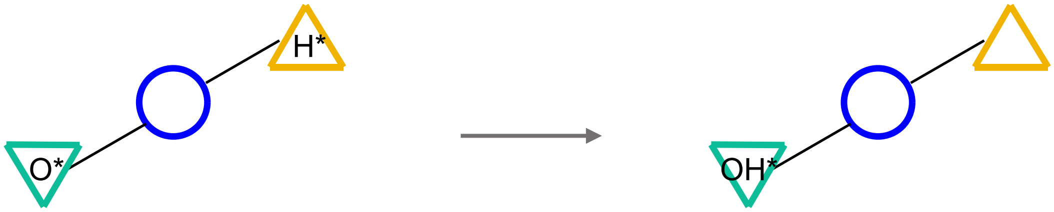

### 13. $H_2O$* formation

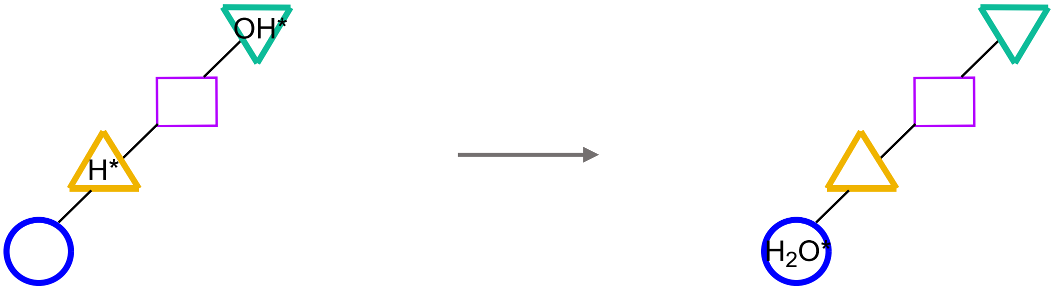

### 14. $H_2O$* formation + O*

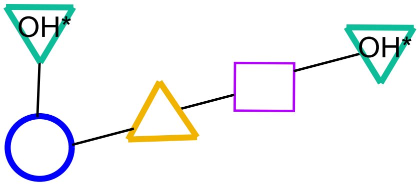

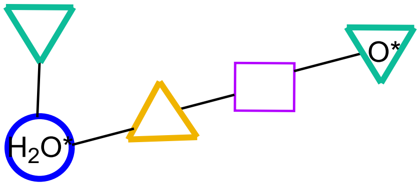

A pairwise O–O lateral interaction with an interaction energy equal to 0.121 eV calculated at DFT level for two O* on adjacent hcp sites, due to the poisoning of the surface. Moreover, at higher temperatures (800 K - 1023 K), since the C* coverage is high, the pairwise C–C lateral interaction was included in the simulations, taking an interaction energy equal to 0.424 eV for two nearby C* atoms adsorbed on hcp sites.

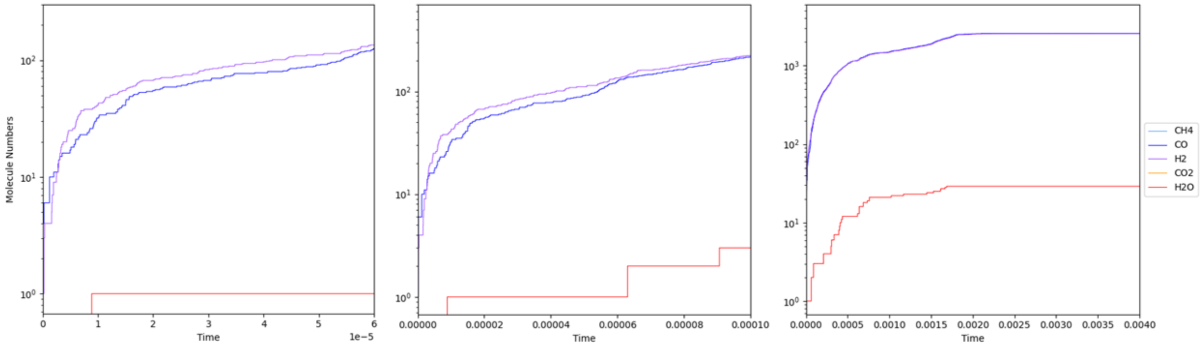

**Figure S5:** Number of molecules of produced products at a logarithmic scale as a function of time (in seconds) for a *k*MC simulation at 973 K and 100 kPa of total pressure at different simulation times to observe the change of the ratio $H_2$/CO production until the steady state is reached.

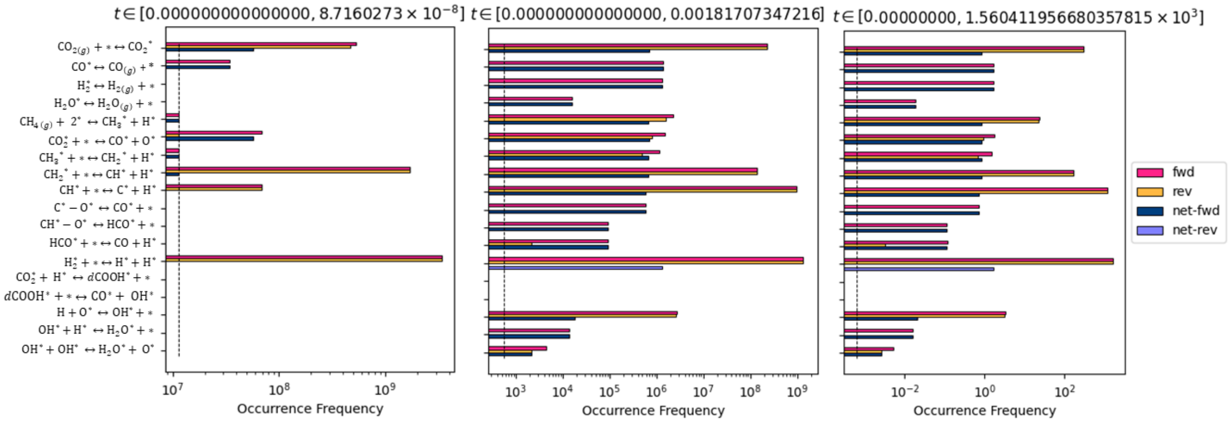

**Figure S6:** Main elementary processes and their frequencies per site (in $s^{-1}$) during different stages for a *k*MC simulation at 973 K and 100 kPa of total pressure. Early stage (on the left), stage used to obtain the TOF (in the middle) and steady state (on the right). A similar trend is found for all *k*MC simulations.

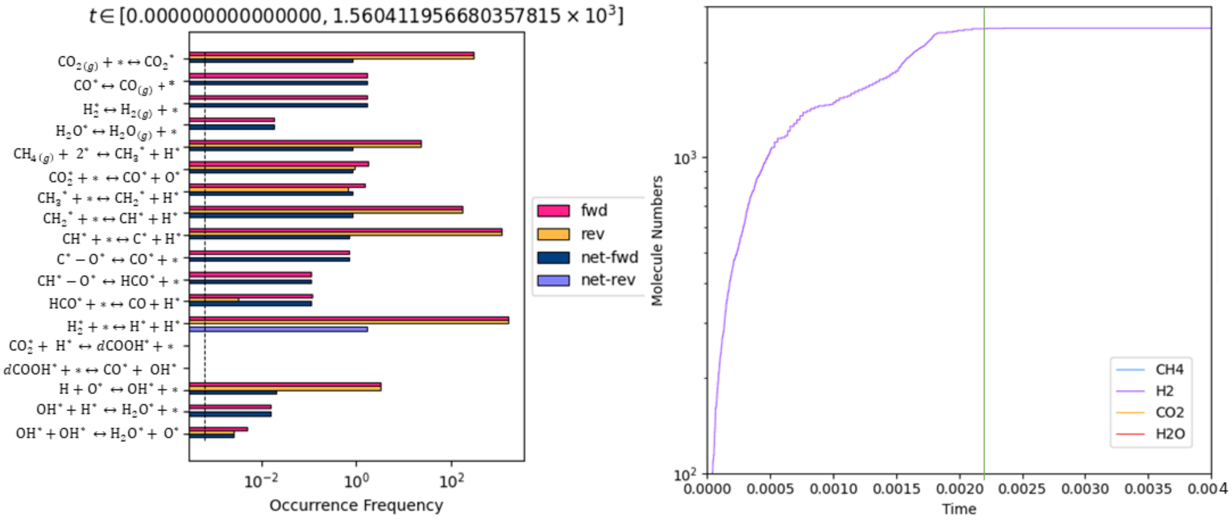

**Figure S7.** Main elementary processes and their frequencies for the DRM at Ru (0001) at $P_{CO2}$ = 50 kPa, $P_{CH4}$ = 50 kPa, and T = 973.15 K for an initial ratio $CH_4/CO_2$ 1:1 for a total simulation time equal to $1.6 \cdot 10^3$ seconds. The green line represents approximately when the catalyst deactivates due to poisoning.

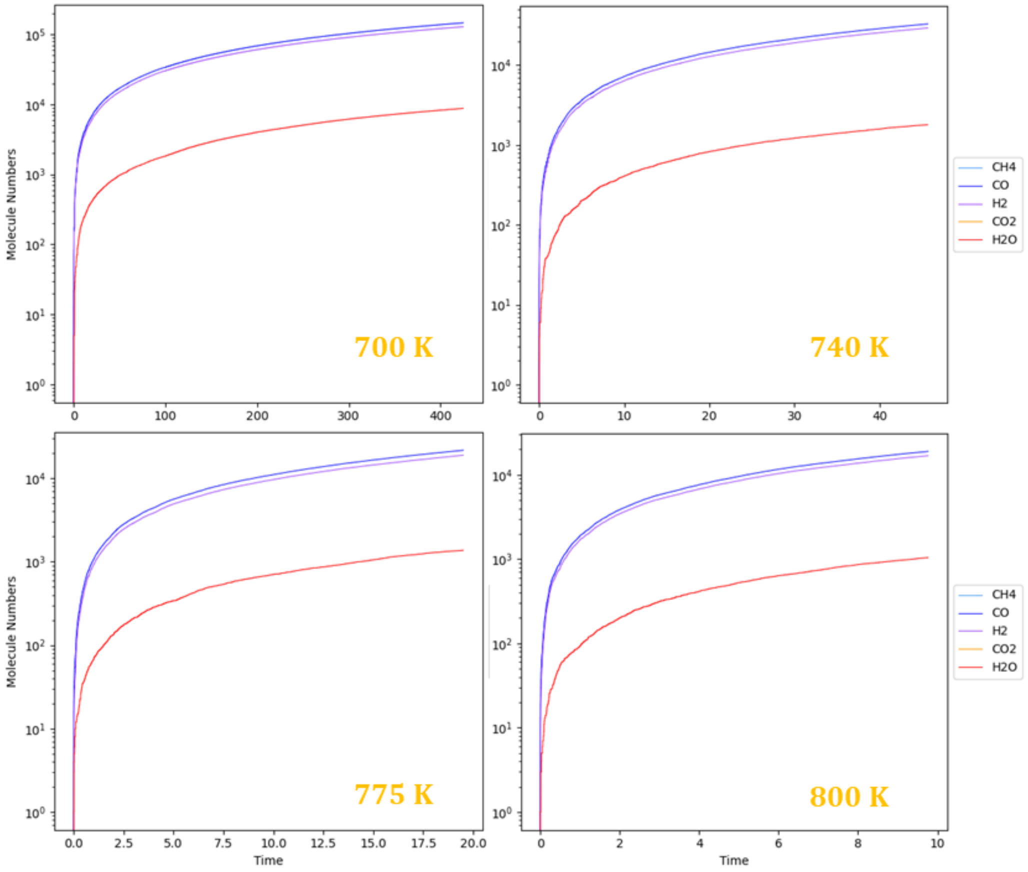

**Figure S8:** Major and minor products of the DRM reaction catalyzed by Ru (0001) at different temperatures and a total pressure of 0.32 kPa.

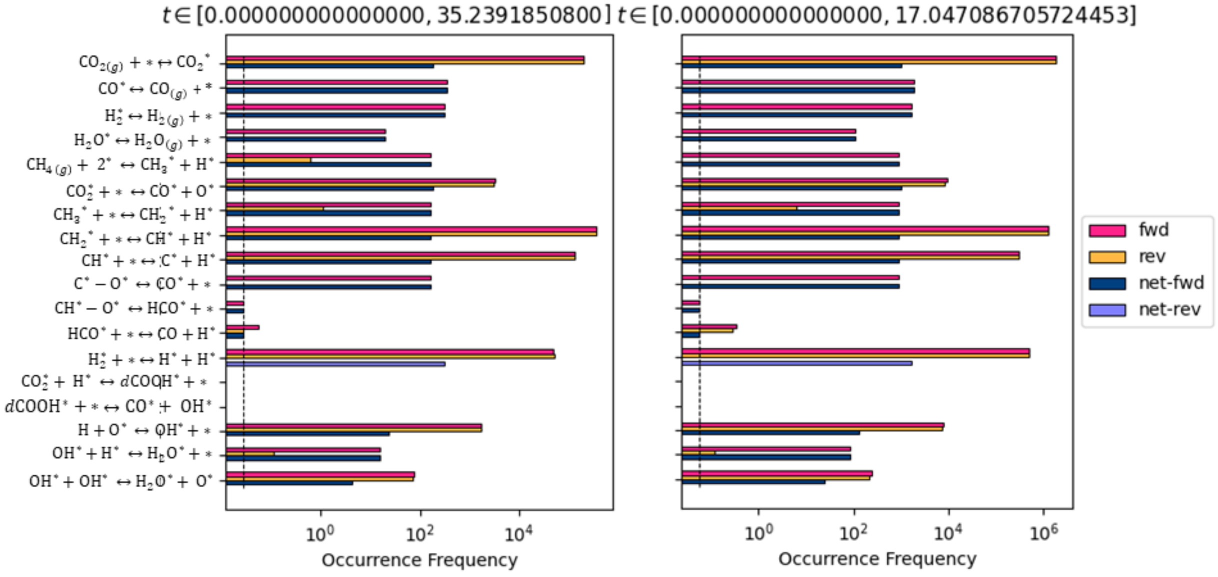

**Figure S9.** Comparison of the main elementary processes and their frequencies for the DRM at Ru (0001) at $P_{CH_4}$= 0.16 kPa and $P_{CO_2}$= 0.16 kPa and T = 700 K (left) and T = 800 K (right) and at the simulation time where the less frequent processes start taking place.

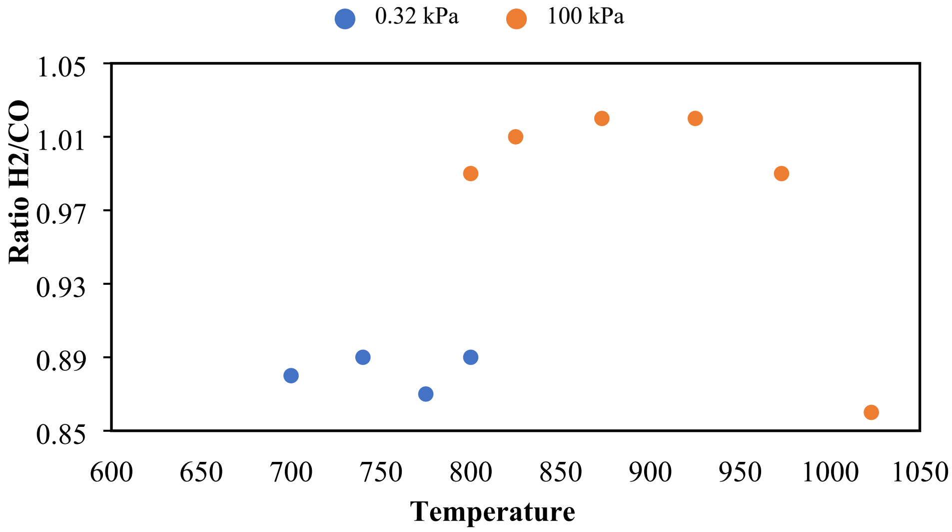

**Figure S10:** $H_2$/CO ratio for both regimes of temperature, 700-800 K and 0.32 kPa (blue) and 800-1023 K and 100 kPa (orange).

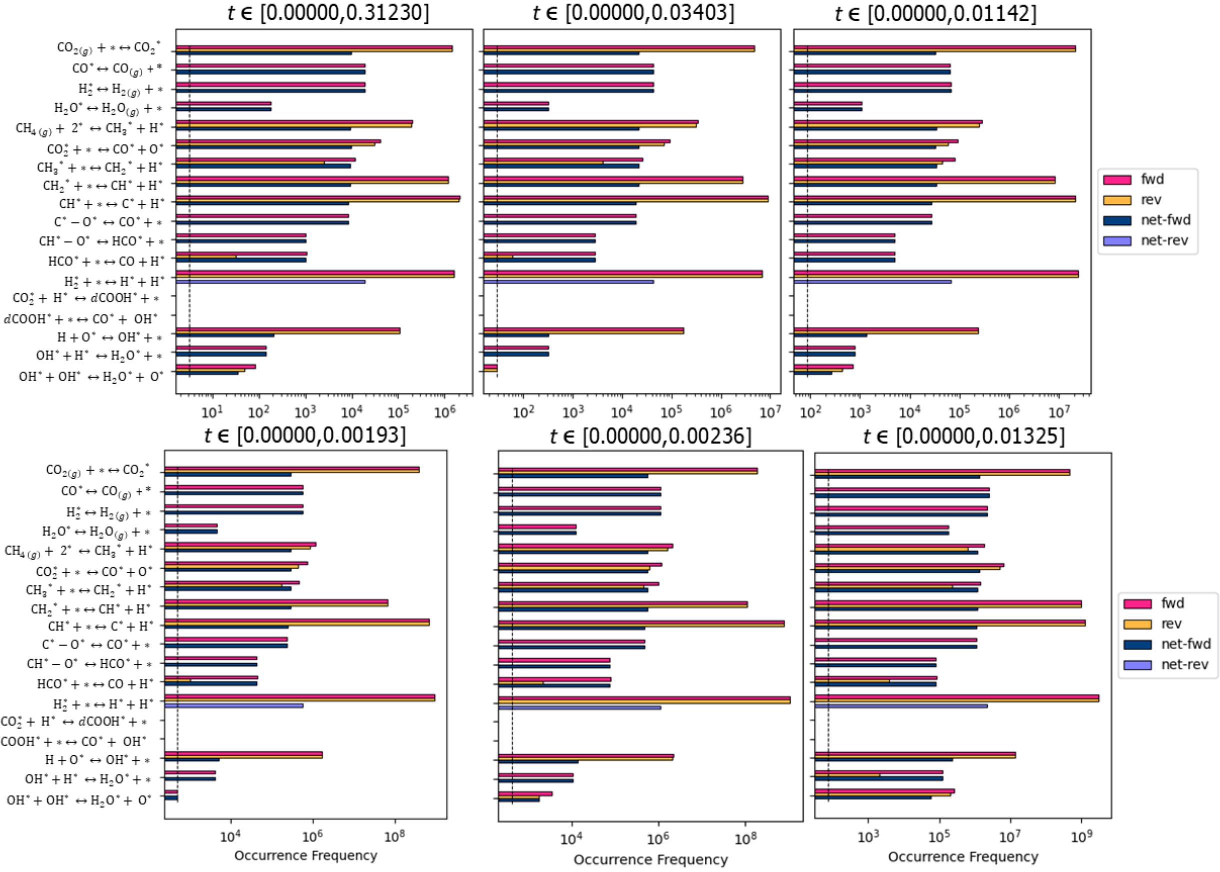

**Figure S11:** Main elementary processes and their frequencies for the DRM on Ru (0001) at $P_{CO2}$ = 50 kPa, $P_{CH4}$ = 50 kPa, and temperatures from 800 K to 1023K for an initial ratio $CH_4/CO_2$ 1:1 before the steady state is reached.

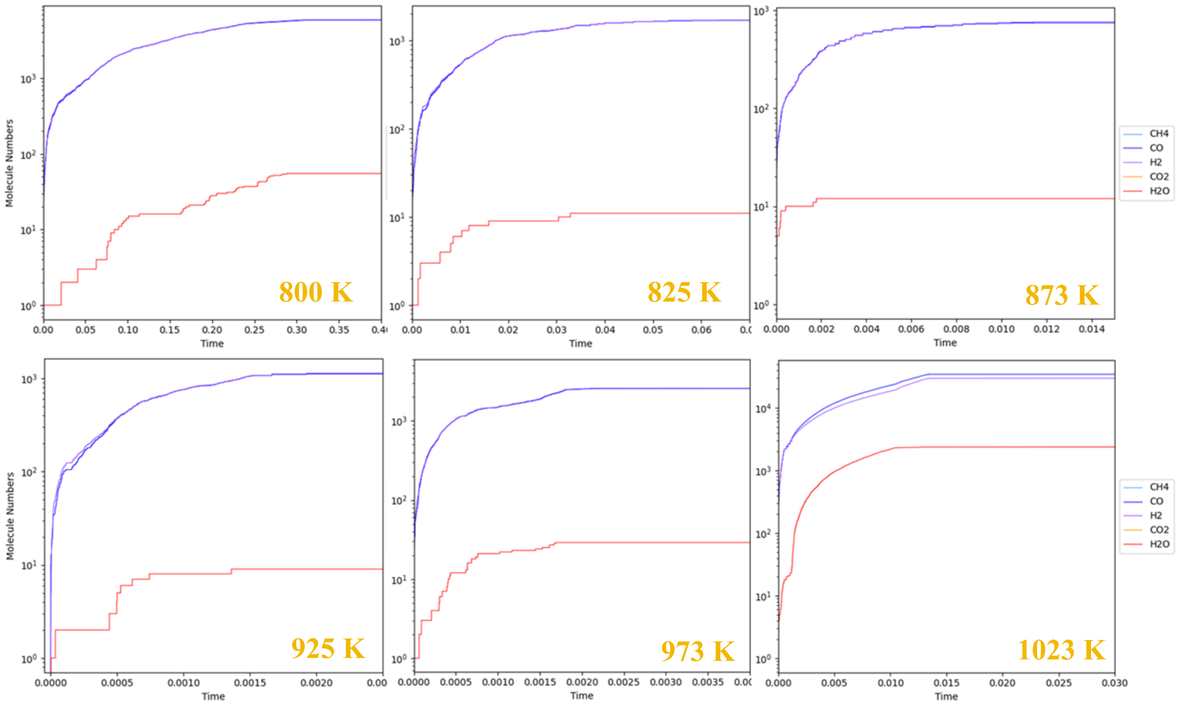

**Figure S12:** Number of molecules of produced products using a logarithmic scale as a function of time (in seconds) for the DRM on Ru (0001) at $P_{C02}$ = 50 kPa, $P_{CH4}$ = 50 kPa, and temperatures from 800 K to 1023K for an initial ratio $CH_4/CO_2$ 1:1.

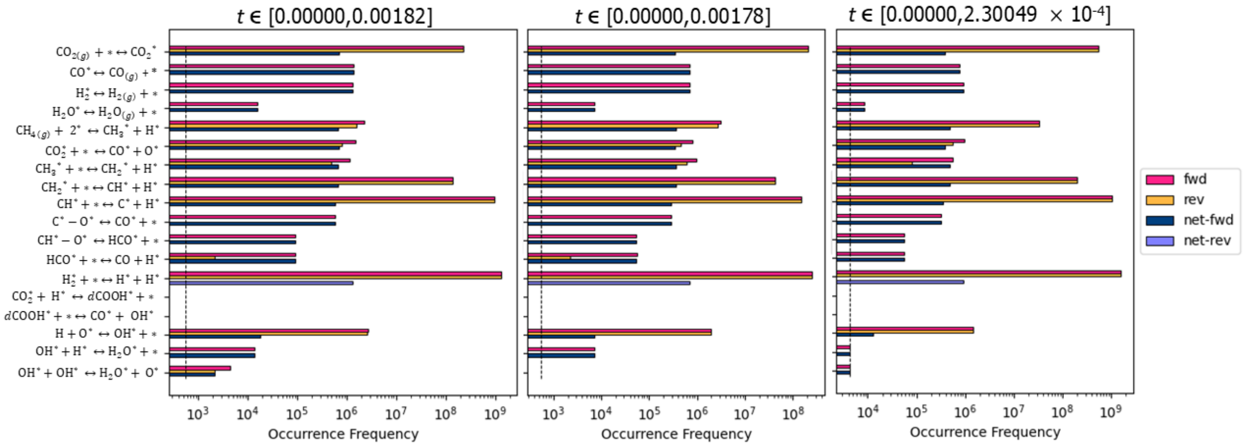

**Figure S13:** Main elementary processes and their frequencies for the DRM on Ru (0001) at 973 K of temperature and 100, 1000 and 1500 kPa of pressure, respectively for an initial ratio $CH_4/CO_2$ 1:1 and for simulation times before the respective steady states are reached.

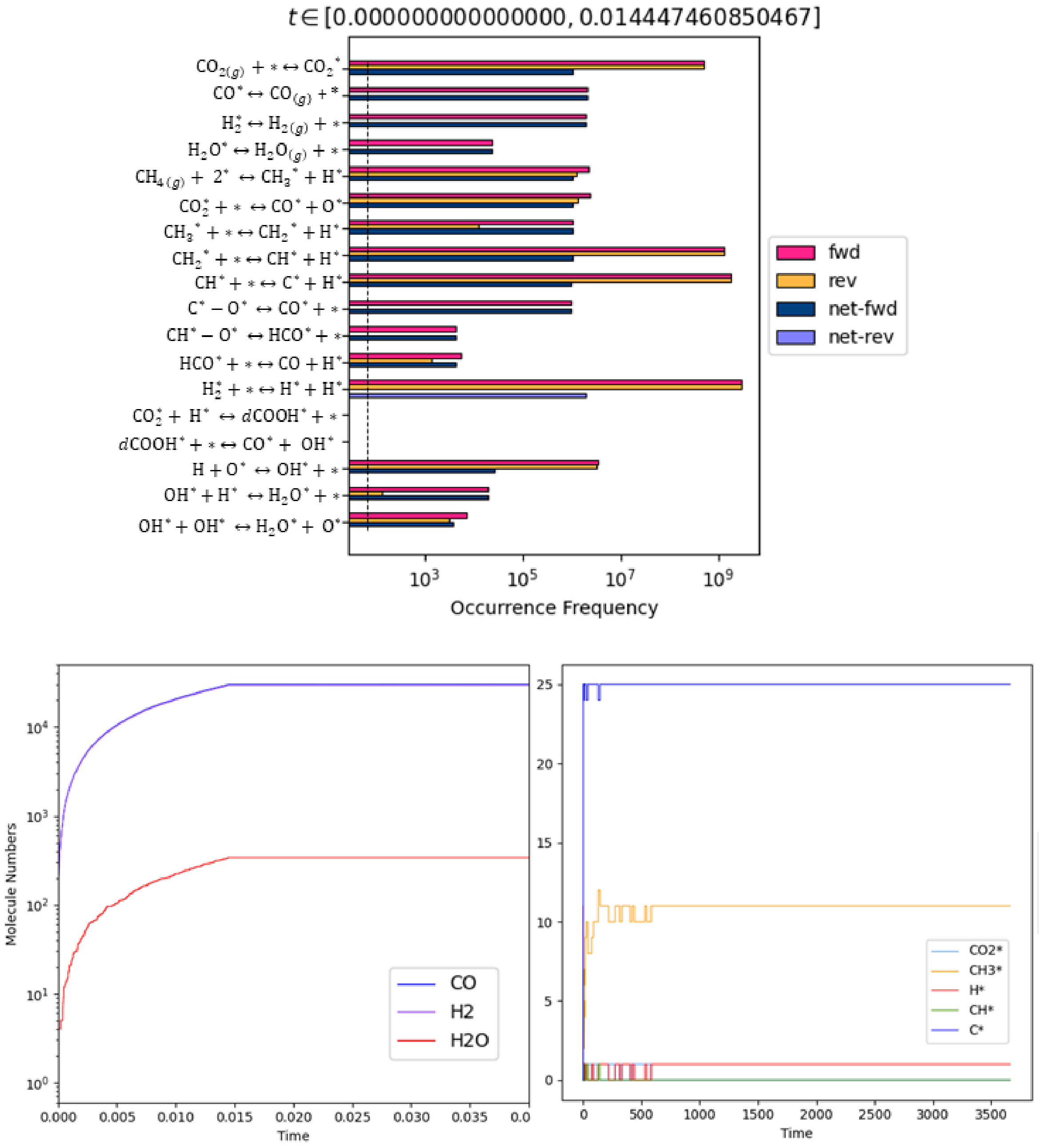

**Figure S14:** Main elementary processes and their frequencies (top) for the DRM on Ru (0001) at 973 K of temperature and 100 kPa of pressure for an initial ratio $CH_4/CO_2$ 1:1 before reaching the steady-state. The number of molecules produced (bottom, left) and coverage (bottom, right) under 973 K of temperature and 100 kPa of pressure without the C-C interaction included.

## Supporting note 1: Thermodynamics

The thermodynamic properties of isolated molecules and adsorbates were calculated at standard conditions, the standard state was defined as 1 bar pressure and at coverage of adsorbed species corresponding to one adsorbate/unit cell (low coverage). We estimated the free energy of gas-phase species by considering translational, rotational, and vibrational degrees of freedom. All the degrees of freedom of adsorbed species, including TSs, were treated as vibrational within the harmonic approximation and later treated within the framework of statistical mechanics. We did not consider thermal effects on metal atoms. We constructed the Reaction (free) energy diagrams and (free) energy barriers by assuming an infinite separation between co-adsorbed species, i.e., the energy of co-adsorbed species is equal to the sum of the individual adsorption energies (at low coverage).

According to our experience, the gas-phase electronic energy for CO molecule is not well represented within our DFT calculations and is the main source of error in gas-phase thermochemistry for the evaluated reactions. By just correcting the electronic energy value of CO molecule (reduction of *ca.* 40 kJ/mol), we reproduced the experimental gas-phase thermodynamics for the Dry Reforming of Methane (DRM) reaction. It is worth mentioning that the CO adsorption energy is commonly corrected in the literature.[1,2]

## Supporting note 2: Kinetic Monte Carlo Modeling

Kinetic Monte Carlo modeling simulations were performed using the Zacros software version 2.0. The thermodynamic parameters entering the *k*MC simulations were obtained from periodic DFT calculations treated within the framework of statistical mechanics treatment. In the case of isolated gas-phase species the entropic corrections were calculated with Gaussian 09. The formation energies of the molecular species/configurations are defined as the required or released energy for generating that configuration from the reference set, which is {a clean Ru (0001) surface, $CO_{(g)}$, $CH_{4(g)}$, and $H_{2(g)}$}. All energy values include the zero-point energy (ZPE) contribution, calculated by considering both the gas and adsorbed phases within the harmonic approximation.

**Table S1**: Turnover frequency, number of molecules for major and minor products and main adsorbed species on Ru (0001) surface at temperature range 700-800 K and 800-1023 K.

| *P* (kPa) | Temperature (K) | Number of molecules | | | Ratio ($H_2$/CO) | Time (s) | TOF ($s^{-1}$) | Coverage (hcp sites) | | | $H_2O$/s |
|---|---|---|---|---|---|---|---|---|---|---|---|
| | | $H_2$ | CO | $H_2O$ | | | | O* ML | C* ML | CH* ML | |
| 0.32 | 700 | 200336 | 228063 | 13860 | 0.88 | 6.63E+02 | 2.29 | 0.44 | 0.04 | – | 2.09E+01 |
| | 740 | 29434 | 33072 | 1814 | 0.89 | 4.61E+01 | 4.78 | 0.40 | – | – | 3.94E+01 |
| | 775 | 31365 | 35954 | 2289 | 0.87 | 3.23E+01 | 7.42 | 0.44 | – | – | 7.09E+01 |
| | 800 | 16778 | 18867 | 1038 | 0.89 | 9.74E+00 | 12.9 | 0.36 | – | – | 1.07E+02 |
| 100 | 800 | 5828 | 5900 | 55 | 0.99 | 3.11E-01 | 126 | 0.04 | 0.28 | 0.68 | 1.77E+02 |
| | 825 | 1712 | 1693 | 11 | 1.01 | 6.36E-02 | 177 | – | 0.28 | 0.72 | 1.73E+02 |
| | 873 | 759 | 742 | 12 | 1.02 | 1.14E-02 | 433 | – | 0.28 | 0.72 | 1.05E+03 |
| | 925 | 1142 | 1119 | 9 | 1.02 | 2.46E-03 | 3029 | – | 0.28 | 0.72 | 3.66E+03 |
| | 973 | 2558 | 2575 | 29 | 0.99 | 2.36E-03 | 7284 | – | 0.28 | 0.72 | 1.23E+04 |
| | 1023 | 29486 | 34168 | 2362 | 0.86 | 1.37E-02 | 16643 | – | 0.28 | 0.72 | 1.73E+05 |

## References:

1 L. Foppa, M. C. Silaghi, K. Larmier and A. Comas-Vives, *J. Catal.*, 2016, **343**, 196–207.

2 C. Fan, Y. A. Zhu, M. L. Yang, Z. J. Sui, X. G. Zhou and D. Chen, *Ind. Eng. Chem. Res.*, 2015, **54**, 5901–5913.